

Article

An Elementary Model for a Self-Accelerating Outward Propagating Flame Subject to the Rayleigh–Taylor Instability: Transition to Detonation

Leonid Kagan ^{*,†}  and Gregory Sivashinsky [†]

Sackler Faculty of Exact Sciences, School of Mathematical Sciences, Tel Aviv University, Tel Aviv 69978, Israel; grishas@tauex.tau.ac.il

* Correspondence: kaganleo@tauex.tau.ac.il

† These authors contributed equally to this work.

Received: 29 September 2020; Accepted: 28 October 2020; Published: 31 October 2020



Abstract: Within the Boussinesq approximation, an elementary model for the deflagration-to-detonation transition triggered by self-acceleration of an expanding flame is formulated and explored. The self-acceleration is sustained by the intrinsic Rayleigh–Taylor instability until the Deshaies–Joulin deflagrability threshold is reached, followed by an abrupt transition to detonation. Emergence of the threshold is caused by positive feedback between the accelerating flame and the flame-driven pressure shock that results in the thermal runaway when the flame speed reaches a critical level. The model offers a simple mechanism that may be responsible for the transition to detonation in thermonuclear supernovae.

Keywords: self-accelerating flames; inverse cascade; Rayleigh–Taylor instability; Boussinesq approximation; deflagration-to-detonation transition; supernovae explosions

1. Introduction

Understanding supernovae explosions is a fundamental astrophysical issue that has frustrated theorists since the effect was first clearly identified by Zwicky in 1933, and it is still commonly regarded as an unsolved problem (Röpke [1]). There is a general consensus that the Type Ia supernova explosion of a degenerate carbon white dwarf star is a manifestation of the deflagration-to-detonation transition (DDT) triggered by an outward-propagating thermonuclear flame subjected to Darrieus–Landau (DL) and Rayleigh–Taylor (RT) corrugations causing the flame to accelerate prior to the transition [2].

The present study offers an elementary model of the DDT event by synthesizing a weakly nonlinear equation of the RT-instability with the Deshaies–Joulin (DJ) theory of thermal runaway [3].

Unlike terrestrial chemical flames, in thermonuclear flames the thermal expansion of reaction products is relatively small [1,4–6], which justifies utilization of the Boussinesq distinguished limit [7]. The Boussinesq quasi-constant-density approximation, in turn, suppresses development of the DL-instability, whose impact is generally deemed inferior to that of the RT.

In the DJ analysis [3], the upper bound for the flame speed is caused by positive feedback between the advancing flame and the flame-driven pressure shock that results in the thermal runaway when the flame speed reaches a critical level. The crucial point of the DJ approach is that at the DDT threshold the corrugated flame may stay perfectly subsonic (see also [8–10]). This premise allows one to deal with the small (yet nonzero) Mach number approximation with all the technical advantages it provides. Moreover, the ability of a subsonic flame to trigger the transition challenges the common view that to ensure DDT the flame should cross the threshold of the DJ-deflagration.

2. Modelling

For the Boussinesq limit the appropriately scaled dispersion relation for an upward propagating planar flame reads (see Zeldovich et al. [11], Equation (3.57) at $\alpha \rightarrow 1$, while keeping $(\alpha - 1)g$ finite), (Figure 1):

$$\omega = \frac{1}{2} \left(\sqrt{k^2(k-1)^2 + Gk} - k - k^2 \right) \tag{1}$$

Here k is the perturbation wave-number in units of $1/l_M$, l_M = Markstein length, ω = perturbation growth rate in units of U_b/l_M , U_b = planar flame speed relative to the burned gas under isobaric conditions, $G = 2(\alpha - 1)gl_M/U_b^2$ = buoyancy parameter, α = ratio of unburned to burned gas densities, and g = acceleration due to gravity.

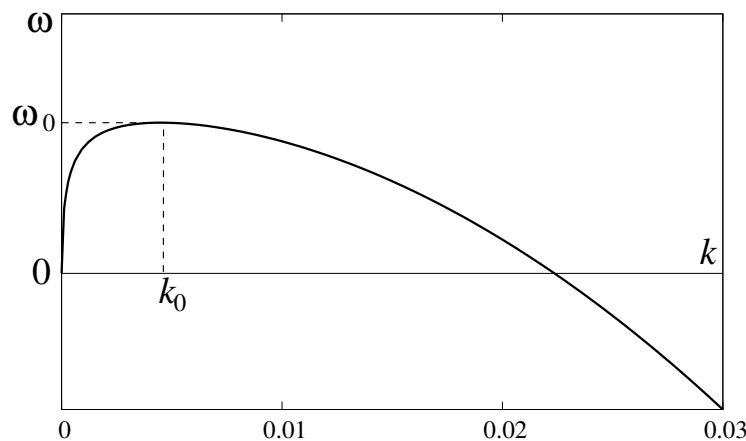


Figure 1. Dispersion relation $\omega(k)$ defined by Equation (1); $G = 0.002$, $k_0 = 0.0045$, $\omega_0 = 0.0004$.

For thermonuclear flames the Lewis number may be regarded as infinitely large [4]. Hence, $l_M = \frac{1}{2}\beta l_{th}$ [11,12], where β = Zeldovich number and l_{th} = flame width.

Similar to the weakly nonlinear equation for the DL-instability [12,13], the analogous equation for an upward-propagating planar flame subjected to the RT-instability may be written as

$$\frac{\partial \Phi^{(0)}}{\partial t} = 1 + \frac{1}{2} \left(\frac{\partial \Phi^{(0)}}{\partial x} \right)^2 + I [\Phi^{(0)}] \tag{2}$$

where

$$I [\Phi^{(0)}] = \sum_{n=1}^{\infty} \omega \left(\frac{2\pi n}{\Lambda} \right) \left\{ \frac{2}{\Lambda} \int_{-\frac{1}{2}\Lambda}^{\frac{1}{2}\Lambda} \Phi^{(0)}(x', t) \cos \left[\left(\frac{2\pi n}{\Lambda} \right) (x - x') \right] dx' \right\} \tag{3}$$

Equations (2) and (3) are considered over a finite interval, $-\Lambda/2 < x < \Lambda/2$, with periodic boundary conditions:

$$\Phi^{(0)} \left(-\frac{1}{2}\Lambda, t \right) = \Phi^{(0)} \left(\frac{1}{2}\Lambda, t \right), \tag{4}$$

$$\Phi_x^{(0)} \left(-\frac{1}{2}\Lambda, t \right) = \Phi_x^{(0)} \left(\frac{1}{2}\Lambda, t \right)$$

Here (x, t) are scaled spatio-temporal coordinates in units of l_M and l_M/U_b , $\Phi^{(0)}$ = flame profile in units of l_M . The superscript in $\Phi^{(0)}$ corresponds to the zero-Mach-number (isobaric) limit.

To accommodate the precompression-induced runaway we adopt the relation suggested by the DJ small-Mach-number approximation [3], (Figure 2).

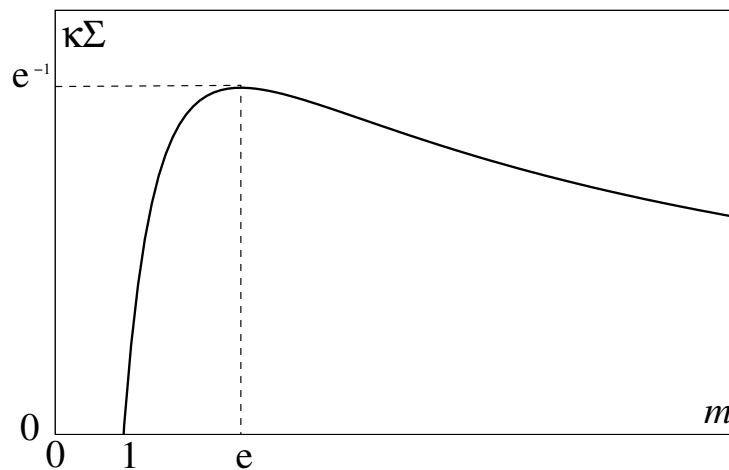


Figure 2. $\kappa\Sigma$ vs. m -dependency defined by Equation (5).

$$\frac{\ln m}{m} = \kappa\Sigma \tag{5}$$

where

$$m = \Phi_t^{(M)} / \Phi_t^{(0)} \tag{6}$$

and

$$\Sigma = 1 + \frac{1}{2} \overline{\left(\Phi_x^{(0)}\right)^2} = \overline{\Phi_t^{(0)}} \tag{7}$$

is the folding factor. The overbar means the average over the channel cross-section.

$$\kappa = \frac{1}{2}\beta(\gamma - 1)\text{Ma} \tag{8}$$

is the compressibility parameter, $\text{Ma} = U_u/a_u$ is the Mach number, $\gamma = c_p/c_v$ is the adiabatic index, and $a_u, U_u = U_b/\alpha$ are sonic and flame velocities relative to the unburned gas. The superscript in $\Phi^{(M)}$ corresponds to the small-Mach-number approximation.

Equation (5) readily implies that at the deflagrability (DDT) threshold, (Figure 2)

$$\kappa\Sigma_{DDT} = e^{-1} \tag{9}$$

Equation (8) pertains to the one-step Arrhenius kinetics and the ideal gas equation of state. For the thermonuclear flame the structure of the compressibility parameter (κ) is more involved (Section 4) but this should not affect the overall dynamical picture.

Following [14], for an outward propagating flame $r = R^{(0)}(\varphi, t)$ Equations (2) and (3) are modified to

$$\frac{\partial R^{(0)}}{\partial t} = 1 + \frac{1}{2R^{(0)2}} \left(\frac{\partial R^{(0)}}{\partial \varphi}\right)^2 + I[R^{(0)}] \tag{10}$$

where

$$I[R^{(0)}] = \frac{1}{\pi} \sum_{n=1}^{\infty} \omega\left(\frac{n}{R^{(0)}}\right) \int_0^{2\pi} \cos[n(\varphi - \varphi')] R^{(0)}(\varphi', t) d\varphi' \tag{11}$$

and

$$\overline{R^{(0)}} = \frac{1}{2\pi} \int_0^{2\pi} R^{(0)}(\varphi, t) d\varphi \tag{12}$$

Solutions of the model (10)–(12) are valid as long as $R^{(0)}(\varphi, t)$ remains positive.

Similarly, Equations (6) and (7) are modified to

$$m = R_t^{(M)} / R_t^{(0)} \tag{13}$$

$$\Sigma = 1 + \frac{1}{2\overline{R^{(0)}}^2} \left(\frac{\partial R^{(0)}}{\partial \varphi} \right)^2 = \frac{\partial R^{(0)}}{\partial t} \tag{14}$$

In Equation (1) for $\omega(n/\overline{R^{(0)}})$ of Equation (11) the buoyancy factor G is treated as a prescribed $\overline{R^{(0)}}$ -independent parameter. This premise, while not holding in stars, is presumably adequate enough for mimicking the impact of buoyancy-induced instability.

For an outward propagating flame Equation (5) may be recast as

$$\frac{\partial R^{(M)}}{\partial t} = \left[1 + \frac{1}{2\overline{R^{(0)}}^2} \left(\frac{\partial R^{(0)}}{\partial \varphi} \right)^2 \right] \exp \left[\kappa \left(\frac{\partial R^{(M)}}{\partial t} \right) \right] \tag{15}$$

This equation may be synthesized with Equation (10) yielding a unified model covering both the RT-instability as well as the deflagrability limit:

$$\frac{\partial R}{\partial t} = \left[1 + \frac{1}{2\overline{R^2}} \left(\frac{\partial R}{\partial \varphi} \right)^2 \right] \exp \left[\kappa \left(\frac{\partial R}{\partial t} \right) \right] + I [R] \tag{16}$$

Note that averaging of Equation (16) over $0 < \varphi < 2\pi$ results in the relation similar to Equation (15), but without the distinction between $R^{(0)}$ and $R^{(M)}$.

3. Numerical Experiments

This section is concerned with numerical simulations of two models based on Equations (10) and (16). Here $\sum_{n=1}^{\infty}$ is naturally replaced by $\sum_{n=1}^N$ with large enough N . The numerical method employed is outlined in our recent study of a related problem [15].

The initial condition is specified as a weighted sum of cosines:

$$R(\varphi, 0) = R_0 + A \sum_{n=1}^{N/2} n^2 \exp(-n/10) \cos(n\varphi + \varphi_n) \tag{17}$$

where A is the normalizing factor and φ_n are produced by the pseudo-random generator (Figure 3).

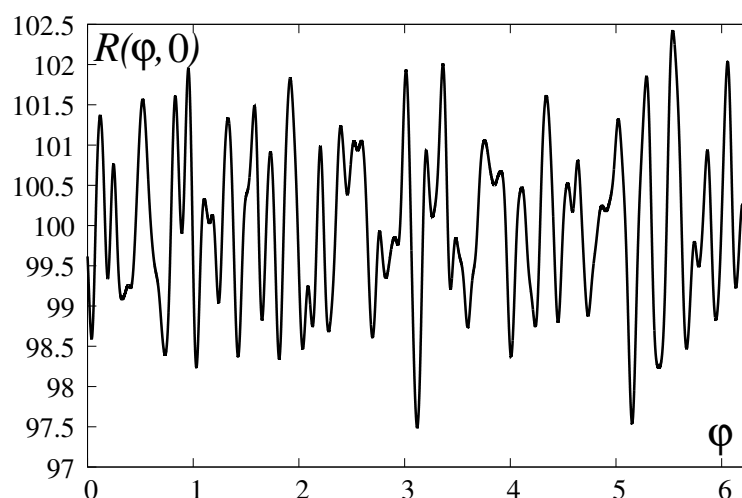


Figure 3. Initial condition $R(\varphi, 0)$ at $A = 0.005$, $R_0 = 100$, $N = 2^{15}$.

Parameters G and κ are specified as $G = 0.002$ and $\kappa = 0.1$, corresponding e.g., to $\alpha = 2$, $\beta = 40$, $g = 2 \cdot 10^9 \text{ cm/s}^2$, $l_{th} = 0.1 \text{ cm}$, $l_M = 2 \text{ cm}$, $U_u = 10^6 \text{ cm/s}$, $U_b = \alpha U_u = 2 \cdot 10^6 \text{ cm/s}$, $Ma = 0.01$, $a_u = 10^8 \text{ cm/s}$, and $\gamma = (4/3 + 5/3)/2 = 1.5$, which are quite realistic [2,4–6].

Figures 4 and 5 show the results of simulations of Equation (10). In the course of its evolution, the flame front assumes a quasi-periodic configuration comprising forward-propagating bubble-like structures trailed by cusps. Small bubbles gradually merge forming larger and faster advancing bubbles, thus exhibiting a strong inverse cascade. The effect was first observed by Vladimirova and Rosner [7] for upward-propagating flames in channels described by a set of Navier–Stokes and advection-diffusion-reaction equations. The inverse cascade effect is also known to occur for flames subjected to the DL-instability but, interestingly enough, not for the diffusively unstable cellular flames [14].

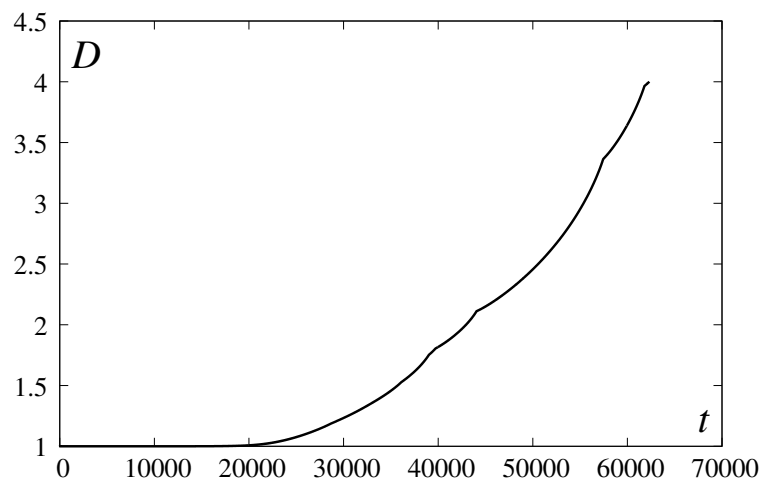


Figure 4. Flame speed $D = \overline{R_t^{(0)}}$ vs. t for the model (10)–(12); $G = 0.002$, $N = 2^{15}$.

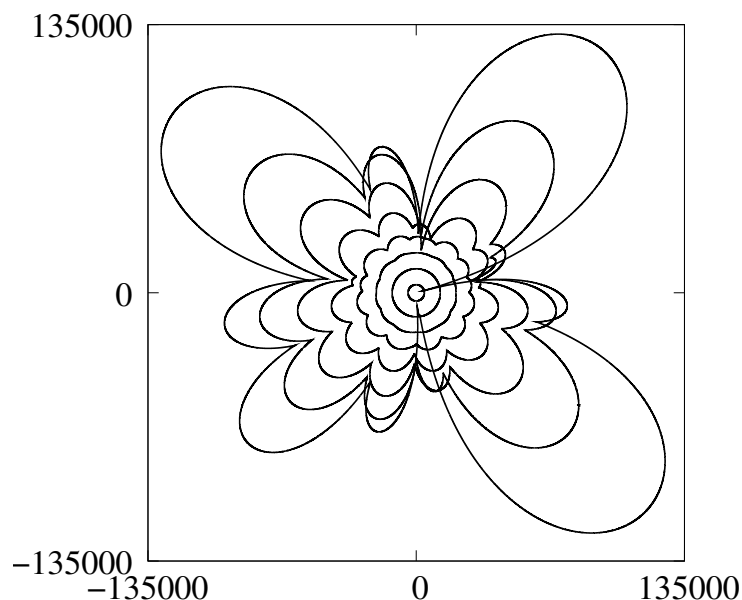


Figure 5. Flame front configurations for the model (10)–(12); $G = 0.002$, $N = 2^{15}$.

Simulation was terminated when rearward moving cusps reached the center ($r = 0$).

At $\kappa = 0.1$ Equation (9) readily yields $\Sigma_{DDT} = D = \bar{R}_t^{(0)} = 3.7$, which in dimensional units corresponds to $7.4 \cdot 10^6$ m/s. Here at the DDT point $t_{DDT} = 6 \cdot 10^4$ (0.06 s) and $\bar{R}_{DDT}^{(0)} = 9.8 \cdot 10^4$ ($1.96 \cdot 10^5$ cm).

Figures 6 and 7 correspond to Equation (16), where the deflagrative mode terminates at $D = \bar{R}_t = 1.9$ ($3.8 \cdot 10^6$ cm/s), $t_{DDT} = 3.5 \cdot 10^4$ (0.035 s), and $\bar{R}_{DDT}^{(0)} = 4.3 \cdot 10^4$ ($8.6 \cdot 10^4$ cm). In Figure 7 the last profile corresponds to the deflagrability threshold.

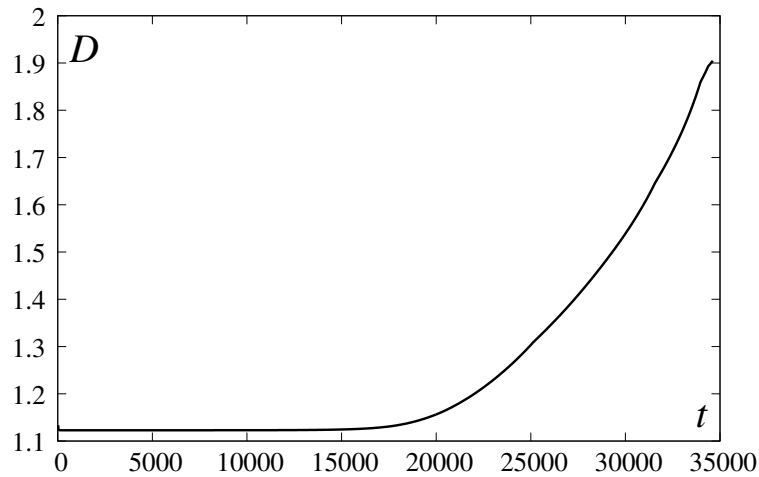


Figure 6. Flame speed $D = \bar{R}_t$ vs. t for the model (11) (12) (16); $G = 0.002$, $\kappa = 0.1$, $N = 2^{15}$.

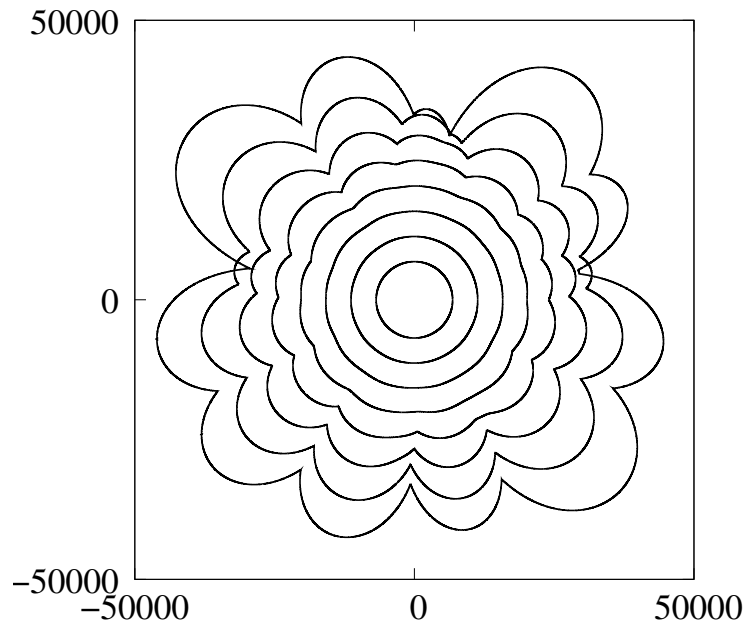


Figure 7. Flame front configurations for the model (11) (12) (16); $G = 0.002$, $\kappa = 0.1$, $N = 2^{15}$.

Occurrence of the inverse cascade is most graphically manifested in the channel geometry.

Figures 8 and 9 depict the developing solution of Equations (2)–(4) for $\Lambda = 80,000$. The incipient multi-bubble structure of the accelerating flame gradually disappears, yielding a single dome-like configuration propagating at a constant velocity.

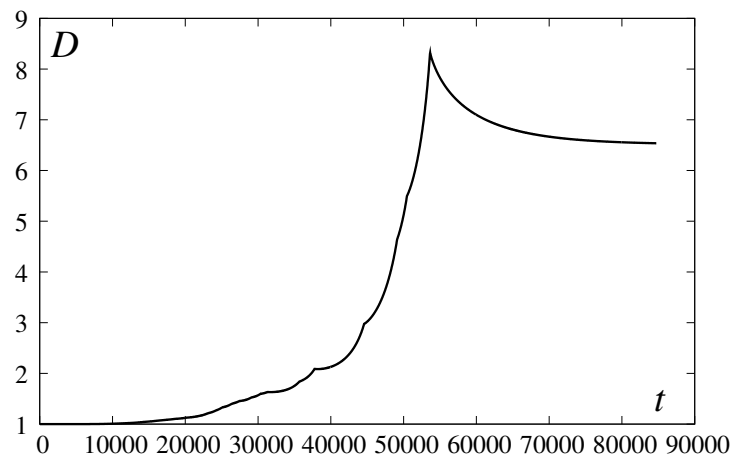


Figure 8. Flame speed $D = \Phi_t^{(0)}$ vs. t for the model (2)–(4); $G = 0.002$, $\Lambda = 80,000$, $N = 2^{15}$.

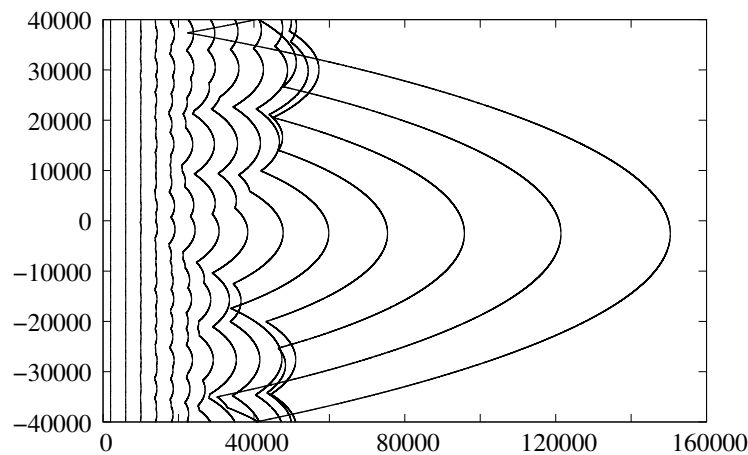


Figure 9. Flame front configurations for the model (2)–(4); $G = 0.002$, $\Lambda = 80,000$, $N = 2^{15}$.

4. Concluding Remarks

1. The proposed weakly nonlinear models are certainly unable to capture the full morphology of the RT-mushrooming [7]. Yet, the models proved adequate enough to imitate the buoyancy-induced corrugations, the inverse cascade, self-acceleration of the front, and occurrence of the deflagrability threshold—the precursor of DDT.
2. Due to the constancy of the buoyancy factor kept at $G = 0.002$, the spatio-temporal scales \bar{R}_{DDT} and t_{DDT} are likely to be grossly underestimated. Accounting for G vanishing at $R \rightarrow 0$ is expected to yield much larger numbers.
3. The gap between deflagrability limits based on Equations (9), (10) and (16) is quite significant but is likely to decrease with a diminishing κ .
4. Our preliminary exploration of the problem for one-step nuclear reaction kinetics and the equation of state for the degenerate electron gas shows that in this case the structure of the compressibility parameter κ is much more involved. This, however, does not affect the form of Equation (16) and the associated dynamical picture.

Author Contributions: Conceptualization, G.S.; methodology, L.K.; software, L.K.; validation, L.K.; formal analysis, G.S.; investigation, G.S.; resources, G.S.; data curation, L.K.; writing—original draft preparation, G.S.; writing—review and editing, G.S.; visualization, L.K.; supervision, G.S.; project administration, G.S.; funding acquisition, G.S. All authors have read and agreed to the published version of the manuscript.

Funding: These studies were supported by the US-Israel Binational Science Foundation (Grant 2012-057) and the Israel Science Foundation (Grant 335/13).

Acknowledgments: This paper is dedicated to the memory of Vitaly Bychkov (1968–2015), a friend and colleague, who has left a legacy of important theoretical works on combustion waves in terrestrial and stellar systems.

Conflicts of Interest: The authors declare no conflict of interest.

References

1. Röpke, F.K. Combustion in thermonuclear supernovae explosions. In *Handbook of Supernovae*; Springer: Cham, Switzerland, 2017.
2. Oran, E.S. Astrophysical combustion. *Proc. Combust. Inst.* **2005**, *30*, 1823–1840. [[CrossRef](#)]
3. Deshaies, B.; Joulin, G. Flame-speed sensitivity to temperature changes and the deflagration-to-detonation transition. *Combust. Flame* **1989**, *77*, 201–212. [[CrossRef](#)]
4. Timmes, F.X.; Woosley, S.E. The conductive propagation of nuclear flames, I. Degenerate C+O and O+Ne+Mg white dwarfs. *Astrophys. J.* **1992**, *396*, 649–667. [[CrossRef](#)]
5. Bychkov, V.V.; Liberman, M.A. Thermal instability and pulsations of the flame front in white dwarfs. *Astrophys. J.* **1995**, *451*, 711–716. [[CrossRef](#)]
6. Poludnenko, A.Y.; Chambers, J.; Ahmed, K.; Gamezo, V.N.; Taylor, B.D. A unified mechanism for unconfined deflagration-to-detonation transition in terrestrial chemical systems and type Ia supernovae. *Science* **2019**, *366*, eaau 7365. [[CrossRef](#)] [[PubMed](#)]
7. Vladimirova, N.; Rosner, R. Model flames in the Boussinesq limit: The effect of feedback. *Phys. Rev. E* **2003**, *67*, 0066305. [[CrossRef](#)] [[PubMed](#)]
8. Koksharov, A.; Bykov, V.; Kagan, L.; Sivashinsky, G. Deflagration-to-detonation transition in an unconfined space. *Combust. Flame* **2018**, *195*, 163–169. [[CrossRef](#)]
9. Gordon, P.V.; Kagan, L.; Sivashinsky, G. Parametric transition from deflagration to detonation revisited: Planar geometry. *Combust. Flame* **2020**, *211*, 465–476. [[CrossRef](#)]
10. Koksharov, A.; Kagan, L.; Sivashinsky, G. Deflagration-to-detonation transition in an unconfined space: Expanding hydrogen-oxygen flames. *Proc. Combust. Inst.* **2020**, *38*, to appear. [[CrossRef](#)]
11. Zeldovich, Y.B.; Barenblatt, G.I.; Librovich, V.B.; Makhviladze, G.M. *The Mathematical Theory of Combustion and Explosions*; Plenum: New York, NY, USA, 1985.
12. Sivashinsky, G.I. Nonlinear analysis of hydrodynamic instability in laminar flames. Part 1. Derivation of basic equations. *Acta Astronaut.* **1977**, *4*, 1177–1206. [[CrossRef](#)]
13. Michelson, D.M.; Sivashinsky, G.I. Nonlinear analysis of hydrodynamic instability in laminar flames. Part 2. Numerical experiments. *Acta Astronaut.* **1977**, *4*, 1207–1221. [[CrossRef](#)]
14. Filyand, L.; Sivashinsky, G.I.; Frankel, M.L. On self-acceleration of outward propagating wrinkled flames. *Phys. D Nonlinear Phenom.* **1994**, *72*, 110–118. [[CrossRef](#)]
15. Kagan, L.; Sivashinsky, G. Modelling of outward propagating flames subjected to Darrieus-Landau and Rayleigh-Taylor instabilities: Transition to detonation. *Combust. Theory Model.* **2020**, submitted.

Publisher's Note: MDPI stays neutral with regard to jurisdictional claims in published maps and institutional affiliations.



© 2020 by the authors. Licensee MDPI, Basel, Switzerland. This article is an open access article distributed under the terms and conditions of the Creative Commons Attribution (CC BY) license (<http://creativecommons.org/licenses/by/4.0/>).